

Edit360: 2D Image Edits to 3D Assets from Any Angle

Junchao Huang¹ Xinting Hu² Shaoshuai Shi⁴ Zhuotao Tian³ Li Jiang^{1,†}

¹The Chinese University of Hong Kong, Shenzhen

²Nanyang Technological University

³Harbin Institute of Technology, Shenzhen

⁴Voyager Research, Didi Chuxing

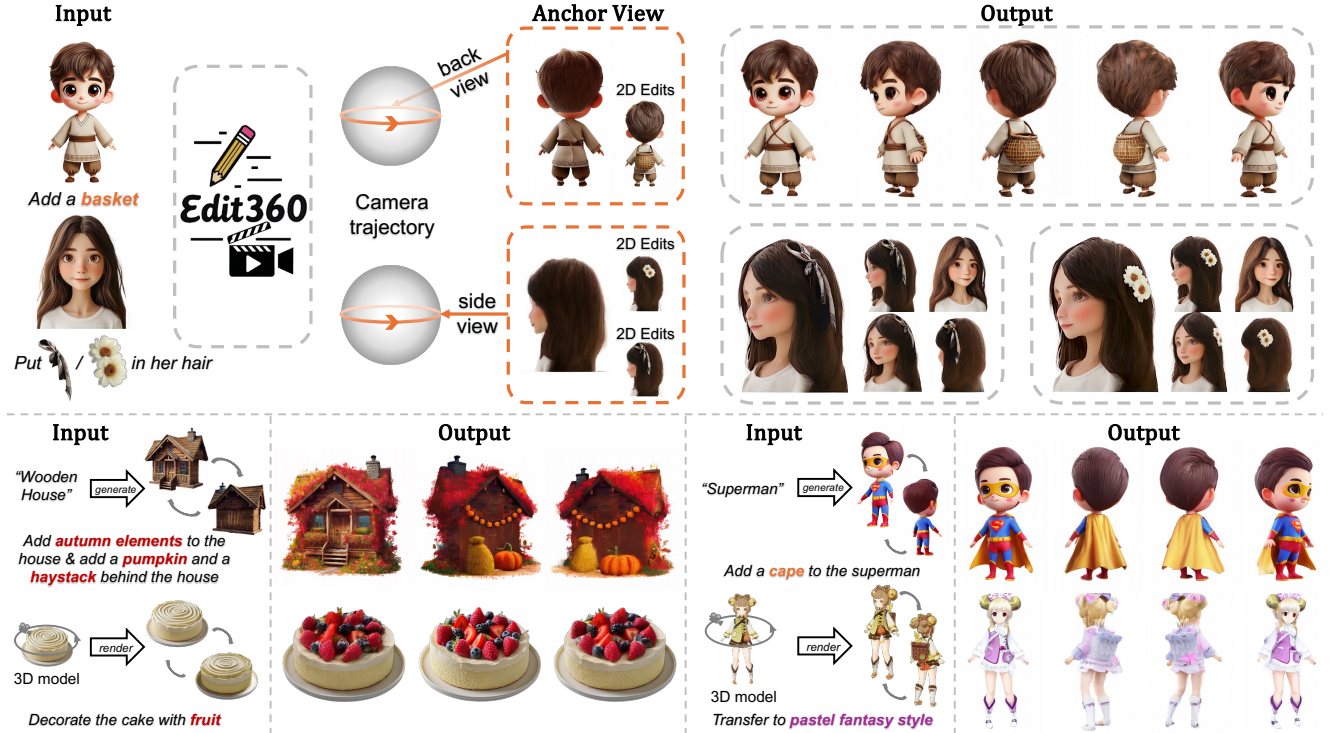


Figure 1. Edit360 enables propagation of 2D edits from any viewpoint to 3D assets, preserving geometric consistency and visual coherence across all views. The framework supports various user inputs, including text descriptions, reference images, and existing 3D assets, allowing for precise and customizable 3D editing. Project page at <https://junchao-cs.github.io/Edit360-demo/>.

Abstract

Recent advances in diffusion models have significantly improved image generation and editing, but extending these capabilities to 3D assets remains challenging, especially for fine-grained edits that require multi-view consistency. Existing methods typically restrict editing to predetermined viewing angles, severely limiting their flexibility and practical applications. We introduce Edit360, a tuning-free framework that extends 2D modifications to multi-view consistent 3D editing. Built upon video diffusion models, Edit360 enables user-specific editing from arbitrary viewpoints while ensuring structural coherence across all views.

[†]Corresponding authors.

The framework selects anchor views for 2D modifications and propagates edits across the entire 360-degree range. To achieve this, Edit360 introduces a novel Anchor-View Editing Propagation mechanism, which effectively aligns and merges multi-view information within the latent and attention spaces of diffusion models. The resulting edited multi-view sequences facilitate the reconstruction of high-quality 3D assets, enabling customizable 3D content creation.

1. Introduction

Diffusion models [16, 40] have revolutionized image generation [36, 38] and editing [60], enabling high-quality creations based on textual descriptions or image inputs, de-

tailed local edits [3], and style transformations [21, 37, 49]. However, extending these capabilities to 3D remains challenging, particularly for fine-grained edits that require consistent propagation of edits across all viewpoints.

Recent advancements in 3D asset generation leverage diffusion models to enhance visual quality, significantly improving texture details and realism [9, 23, 25, 27, 29, 30, 33, 46, 52, 53]. Score Distillation Sampling (SDS)-based methods [23, 33, 52] optimize 3D representations with 2D priors but often suffer from slow convergence, view inconsistency, and the “Janus problem”. Fine-tuning approaches [25, 27, 29] improve cross-view coherence but remain limited by sparse-view training, making consistent edits propagation across multiple views challenging.

In contrast, Video 3D Diffusion Models (V3DMs) [6, 48] generate consistent dense view sequences following the pre-defined camera trajectory from a single front-view image. This property makes them well-suited for editing tasks, as modifications made to one view can be naturally propagated across others. However, current V3DMs are constrained to single front-view inputs, allowing edits only on the front view before generation. This limitation prevents modifications of occluded or less-visible regions. Directly editing alternative viewpoints (e.g., the side/back view) and replacing the original input view results in the loss of identity information provided by the front view. This challenge motivates the development of an approach that enables precise edits tailored to any chosen viewpoint, while maintaining global structural coherence and original identity information.

We introduce Edit360, a tuning-free framework for multi-view consistent 3D editing based on V3DMs. Unlike prior methods constrained to front-view modifications, Edit360 enables user-specified edits from any viewpoint while preserving the asset’s global identity and structure. Given a user-provided editing instruction, Edit360 selects anchor views, which are the most suitable perspectives for a given edit. After performing precise 2D modifications on these anchor views using off-the-shelf image editing models [49, 60], Edit360 propagates these edits across all viewpoints through the proposed Anchor-View Editing Propagation mechanism. This approach ensures that local edits remain structurally and semantically coherent across the entire 360-degree range while preserving the identity of the object in the reconstructed 3D asset.

Anchor-View Editing Propagation extends current V3DMs by introducing an additional camera trajectory starting from the anchor view. This propagation mechanism consists of two complementary components: Spatial Progressive Fusion (SPF) and Cross-View Alignment (CVA). SPF aligns these two trajectories through circular-shift operations and progressively merges them using proximity-based weighting, while CVA enforces structural coherence by injecting structural priors through cross-view attention

mechanisms to prevent artifacts when conflicting details arise. This integrated approach enables Edit360 to preserve user-intended edits specified at arbitrary viewing angles, while maintaining global 3D consistency.

We evaluate Edit360 through qualitative and quantitative analyses. To quantitatively assess multi-view consistency, we integrate an unedited anchor view into the novel-view synthesis process, verifying that its inclusion does not degrade the structural integrity of the 3D model. This confirms that Edit360 seamlessly incorporates multiple anchor views without disrupting the underlying 3D representation. Qualitative results demonstrate that edits applied to the anchor view propagate effectively across all viewpoints, ensuring spatially consistent modifications. These findings validate Edit360’s ability to propagate 2D edits into fully coherent 3D assets while achieving high generation quality.

Overall, our contributions can be summarized as follows:

- We introduce Edit360, a tuning-free framework for multi-view consistent 3D editing, enabling fine-grained modifications from any viewing angle of 3D assets.
- We propose Anchor-View Editing Propagation with Spatial Progressive Fusion (SPF) and Cross-View Alignment (CVA) components, enabling seamless propagation of edits across dense viewpoints with structural coherence.
- Comprehensive experiments demonstrate that Edit360 achieves state-of-the-art performance across diverse tasks, including precise 3D editing from multiple viewpoints, global style transformation, and multi-view conditional generation.

2. Related Works

Image Diffusion Model for 3D Generation. The task of 3D object generation has long been limited by the scarcity of large-scale 3D datasets, limiting content quality and diversity. DreamFusion [33] addressed this by introducing Score Distillation Sampling (SDS), optimizing 3D representations using pre-trained 2D diffusion models. By leveraging rich priors from large-scale 2D image models, DreamFusion achieved high-quality 3D content without extensive 3D data. However, SDS-based approaches [23, 30, 33, 52, 53] face limitations such as a front-view bias, causing the “multi-face Janus problem”. To overcome this, Zero123 [25] fine-tuned image diffusion models with 3D data, enabling novel views from a single image. However, despite the 3D supervision introduced by Zero123 [25] and its subsequent methods [9, 27, 29], image diffusion-based models still struggle with multiview consistency and can only generate sparse views due to capacity and computational constraints, making it challenging to directly use these views for 3D reconstruction.

Video Diffusion Model for 3D Generation. To mitigate these challenges, video diffusion models [1, 14, 47] have

emerged as a powerful alternative for generating dense, continuous sequences of frames with high inter-frame consistency. ViVid-1-to-3 [22] demonstrated that integrating a pre-trained video diffusion model with multiview generation significantly enhances the consistency of the generated views. In a similar vein, Envision3D [31] proposed a two-stage pipeline where a multiview generation model produces sparse anchor views, which are then interpolated by a fine-tuned video diffusion model to generate dense, consistent views. Models like SV3D [48], V3D [6], and VFusion3D [15] directly fine-tuned video diffusion models to generate smooth 360-degree orbit videos, offering consistent multi-view generation from a single input.

3D Object Editing. Traditional 3D editing methods, including explicit geometric deformations [12, 13, 17, 28, 39, 41, 42, 44, 57, 58], implicit representations [24, 45, 55] like NeRFs [26, 56, 59], and hybrid approaches [5, 32] with data-driven priors, are typically designed for specific objects and scenes, resulting in limited generalization capabilities [34]. These challenges have led to a shift toward using advanced 2D image editing techniques for more intuitive and adaptable 3D customization. Methods like Control3D [4] and Generic 3D [2] enable global control in 3D generation by injecting text or image conditions into a 2D diffusion model, then transferring these conditions across multiple views. While effective for maintaining overall consistency, these methods lack precision for localized edits. Recent work, such as Tailor3D [34], enables the fusion of front and back view 2D local edits into 3D representations, but remain constrained by predetermined viewing angles and limited geometric and texture details.

3. Overall Framework

This section presents the overall framework of Edit360, a novel approach for user-guided 3D asset editing that requires no training or fine-tuning. Section 3.1 introduces background on video diffusion models and dense-view synthesis. Building on these models, Section 3.2 details the Edit360 pipeline. Additionally, we discuss how Edit360 enables edits from any viewpoint.

3.1. Preliminaries

Video Diffusion Models (VDMs) generate a video of N frames, $X^{1:N}$, by progressively denoising an initial Gaussian noise sequence over T timesteps. At each timestep t , the VDM network θ predicts noise $\epsilon_\theta(X_t^{1:N}, t, C)$, where C represents conditioning text or image inputs. The iterative denoising process follows:

$$X_{t-1}^{1:N} = \text{Denoise}(X_t^{1:N}, \epsilon_\theta(X_t^{1:N}, t, C)), \quad (1)$$

where the final output $X_0^{1:N}$ is the generated video $X^{1:N}$.

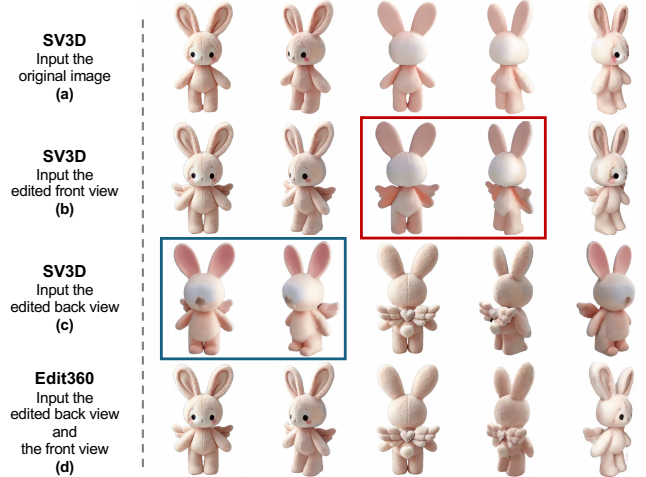


Figure 2. Example of adding wings to a rabbit doll demonstrating the limitations of existing single-view input V3DMs methods (e.g., SV3D [48]) for 3D editing. With only the edited front view as input, SV3D generates incomplete wings that appear fused with the arms (red box). Conversely, using the edited back view as input results in loss of facial identity information (blue box). Our Edit360 approach integrates multi-view information to ensure consistent and complete edits across the entire 3D representation.

Video 3D Diffusion Models (V3DMs) [6, 48] extend VDMs to generate 3D-consistent dense-view sequences by fine-tuning them on novel-view synthesis tasks. Instead of conditioning on the general text or image, V3DMs take a front-view image v^0 as C and predict the sequence of views denoted as: $\{v^0, \dots, v^{N-1}\}$. This sequence represents a full 360-degree orbit around the object along a predefined camera trajectory, where each view v^p corresponds to a view rotated clockwise by $\frac{360}{N} \times p$ degrees relative to v^0 .

3.2. The Pipeline of Edit360

While dense-view synthesis based on Video Diffusion Models (VDMs) can generate high-quality multi-view sequences, their dependence on single-view inputs constrains editing flexibility. For instance, when target edits (such as wings) have limited visibility in the front view, texture and shape inconsistencies emerge in subsequently generated views (Figure 2 (b)). Conversely, performing edits directly in the optimal view for a specific modification (such as the back view where the wing area has maximum visibility) and merely substituting the input view with this edited view results in identity information loss in the reconstructed 3D asset (Figure 2 (c)).

To address these limitations, Edit360 introduces an additional editable anchor view, the optimal view with maximum visibility for the targeted edit. This anchor view can be either manually specified by users or automatically identified using a Large Language Model (LLM). After editing the anchor view, Edit360 employs Anchor-View Editing Propagation mechanism to synchronize the 2D edits

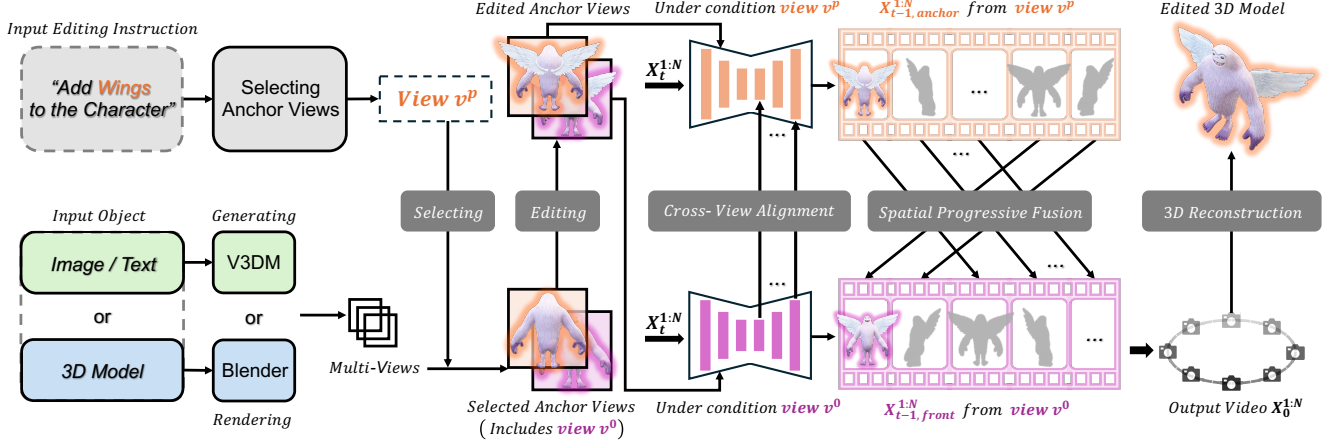


Figure 3. Overview of the Edit360, from input instruction and object (text, image, or 3D model) to the edited 3D asset. With v^p (the back view for this case) selected as the anchor view for editing while v^0 (front view) serving to preserving identity information, our Dual-Stream Diffusion Network progressively generates and fuses multi-view sequences through Spatial Progressive Fusion (SPF) and Cross-View Alignment (CVA) at each sampling step, ensuring consistent view generation for reconstructing the edited 3D asset.

across all views. The mechanism consists of Spatial Progressive Fusion (SPF) and Cross-View Alignment (CVA) to achieve view-consistent editing while maintaining the identity information from the front view. Details are provided in Section 4. This process generates an edited dense-view sequence, which is subsequently used for reconstructing the final edited 3D asset through NeuS [50] or 3DGS [19]. As shown in the bottom row of Figure 2, Edit360 successfully adds geometrically consistent, richly textured wings to the rabbit doll while preserving its facial characteristics. The overall workflow of Edit360 is illustrated in Figure 3.

Multi-Format Input Processing. Edit360 supports diverse formats for editable objects, including text, image, and existing 3D assets. All inputs are standardized into multi-view sequences through format-specific methods: (1) For text inputs, we first synthesize a front view via a text-to-image model [35] then generate multi-views using V3DM [6, 48]; (2) For image inputs, we directly apply V3DM for view synthesis; (3) For existing 3D assets, we use Blender for multi-view rendering.

4. Anchor-View Editing Propagation

To ensure that edits made on the anchor view propagate consistently across the entire dense-view sequence, Edit360 introduces Anchor-View Editing Propagation, a mechanism designed to synchronize modifications across multiple perspectives while preserving global 3D coherence.

In standard V3DMs, the *front-view camera trajectory* is used to generate a dense sequence of views by progressively rotating the camera around the object. The trajectory starts from the front view v^0 and follows a clockwise orbit:

$$X_{\text{front}}^{1:N} = \{v^0, v^1, \dots, v^{N-1}\}, \quad (2)$$

where each view v^p is rotated by $\frac{360}{N} \times p$ degrees relative

to the front view. To enable edits from arbitrary angles, Edit360 first introduces an *anchor-view camera trajectory*, which follows the same camera rotation principle but originates from the user-selected anchor view v^p :

$$X_{\text{anchor}}^{1:N} = \{v^p, v^{p+1}, \dots, v^{(p+N-1) \bmod N}\}. \quad (3)$$

Unlike $X_{\text{front}}^{1:N}$ that remains unedited, $X_{\text{anchor}}^{1:N}$ is generated after modifying the anchor view, ensuring that edits at v^p influence surrounding views.

Anchor-View Editing Propagation aims to progressively fuse these two trajectories, ensuring seamless integration of anchor-view modifications while preserving 3D priors from the front-view trajectory. To achieve this, Edit360 integrates Spatial Progressive Fusion (SPF) to blend the two trajectories through spatial alignment and progressive fusion strategies. Additionally, Cross-View Alignment (CVA) resolves structural inconsistencies between them by enforcing feature-level consistency across corresponding views. These two components work together to perfectly merge the otherwise inconsistent view sequences resulting from anchor-view edits, ensuring that modifications are smoothly propagated across the entire 360-degree sequence while maintaining structural integrity and creating a coherent 3D representation.

4.1. Spatial Progressive Fusion

Spatial Progressive Fusion (SPF) aligns and blends the edited dense views $X_{\text{anchor}}^{1:N}$ along anchor-view camera trajectory with the original $X_{\text{front}}^{1:N}$ along front-view camera trajectory, ensuring smooth propagation of edits while maintaining spatial consistency.

Since each trajectory originates from a different view-point, SPF first aligns the indexed view location of $X_{\text{anchor}}^{1:N}$

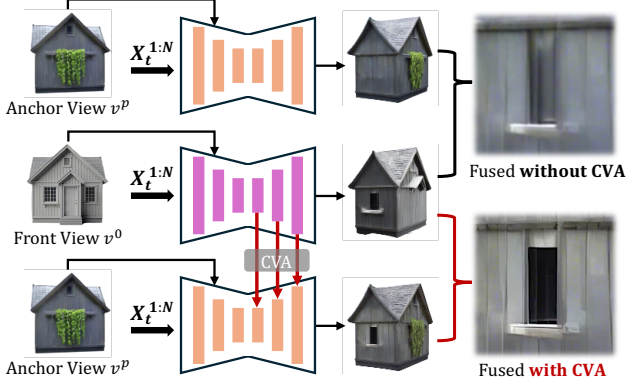


Figure 4. Comparison of fusion results with and without Cross-View Alignment (CVA). The top row shows the result without CVA, where the window is blurred, while the bottom row shows the result with CVA, preserving a clear window in the side view.

to $X_{\text{front}}^{1:N}$. This is achieved using a circular-shift (CS) operation:

$$\text{CS}(X_{\text{anchor}}^i) = X_{\text{anchor}}^{(i+N-p) \bmod N}, \quad i = 0, 1, \dots, N. \quad (4)$$

This alignment ensures that each indexed view i in $\text{CS}(X_{\text{anchor}}^i)$ correspond to the view at the same camera location, where p represents the index of the anchor view.

After alignment, the dense views along two trajectories are merged during each denoising timestep $t \in \{0, 1, \dots, T\}$:

$$X_{t,\text{SPF}}^i = (1 - \alpha^i) \cdot X_{t,\text{front}}^i + \alpha^i \cdot \text{CS}(X_{t,\text{anchor}}^i), \quad (5)$$

where the spatial weight α^i dynamically adjusts the contribution of views from each trajectory based on its proximity to the anchor view. α^i decreases as the cyclic distance between view v_i and the anchor view v_p increases, prioritizing edits in spatial proximity to the anchor view.

In later diffusion stages, SPF integrates edge [18] and texture [11] information to refine structural details and mitigate over-smoothing, ensuring fine-grained consistency across views.

By progressively interpolating between trajectories over multiple timesteps, SPF guarantees that edits introduced in $X_{\text{anchor}}^{1:N}$ are smoothly integrated into $X_{\text{front}}^{1:N}$, maintaining both edit consistency and overall spatial coherence.

4.2. Cross-View Alignment

While Spatial Progressive Fusion (SPF) ensures smooth spatial blending of the front-view and anchor-view trajectories, inconsistencies may still arise due to the inherent randomness of the denoising process. For example, as shown in Figure 4, a side view of a house generated from the front view includes windows, while the same side view generated from the back view lack them. Directly fusing these conflicting results may lead to ghosting artifacts, where struc-

tural details appear blurry or inconsistent (“Fused without CVA” in Figure 4).

To resolve these conflicting structural details, Cross-View Alignment (CVA) enforces feature consistency by using the front-view trajectory $X_{\text{front}}^{1:N}$ as a reference to guide the denoising process of the anchor-view trajectory $X_{\text{anchor}}^{1:N}$. Specifically, CVA injects intermediate features from the front-view denoising process into the anchor-view denoising process using a cross-view feature attention mechanism.

During each denoising step t , we modify the self-attention layers of the diffusion network by injecting key-value pairs from the front-view trajectory into the attention computation of the anchor-view trajectory. The feature-aligned attention output $\mathcal{A}_t^{\text{CVA}}$ is computed as:

$$\mathcal{A}_t^{\text{CVA}} = \text{softmax} \left(\frac{Q_t^a \cdot (K_t^f \oplus K_t^a)^T}{\sqrt{d_k}} \right) \cdot (V_t^f \oplus V_t^a), \quad (6)$$

where \oplus denotes the concatenation operation, d_k is the embedding dimension, Q_t^a , $K_t^{a/f}$, and $V_t^{a/f}$ denote the query, key, and value features from the V3DM along the respective anchor-view (a) or front-view (f) camera trajectory. By injecting front-view priors into the denoising process, CVA guides the model to maintain consistent structure across views, preventing ghosting artifacts while improving geometric fidelity (“Fused with CVA” in Figure 4).

5. Experiments

To demonstrate the effectiveness of our proposed Edit360 framework, we conduct both qualitative and quantitative experiments across 3D editing and generation tasks. Additionally, we perform ablation studies to assess the impact of key components in the Edit360.

5.1. Experimental Setup

Combined with Different V3DMs. Several video 3D diffusion models (V3DMs) [6, 15, 31, 48] fine-tuned on the Objaverse dataset[8] can generate dense views from a single front-view input for 3D reconstruction. We evaluate our method on two representative models: *SV3D^u* [48] generating 21 horizontal views (576×576) and *V3D* [6] producing 18 views (512×512), both at 0-degree elevation. Edit360 extends these V3DMs to support multiple input views without additional training, with all inference performed on a single NVIDIA RTX 4090 GPU.

Datasets and Metrics. For 3D editing tasks, we demonstrated our model’s fine-grained editing capabilities through both qualitative comparisons and quantitative user studies on diverse data sources, including single images (either generated by text-to-image models [35] or captured from the real world) and existing 3D models. For novel multi-view synthesis evaluation, we quantitatively assessed

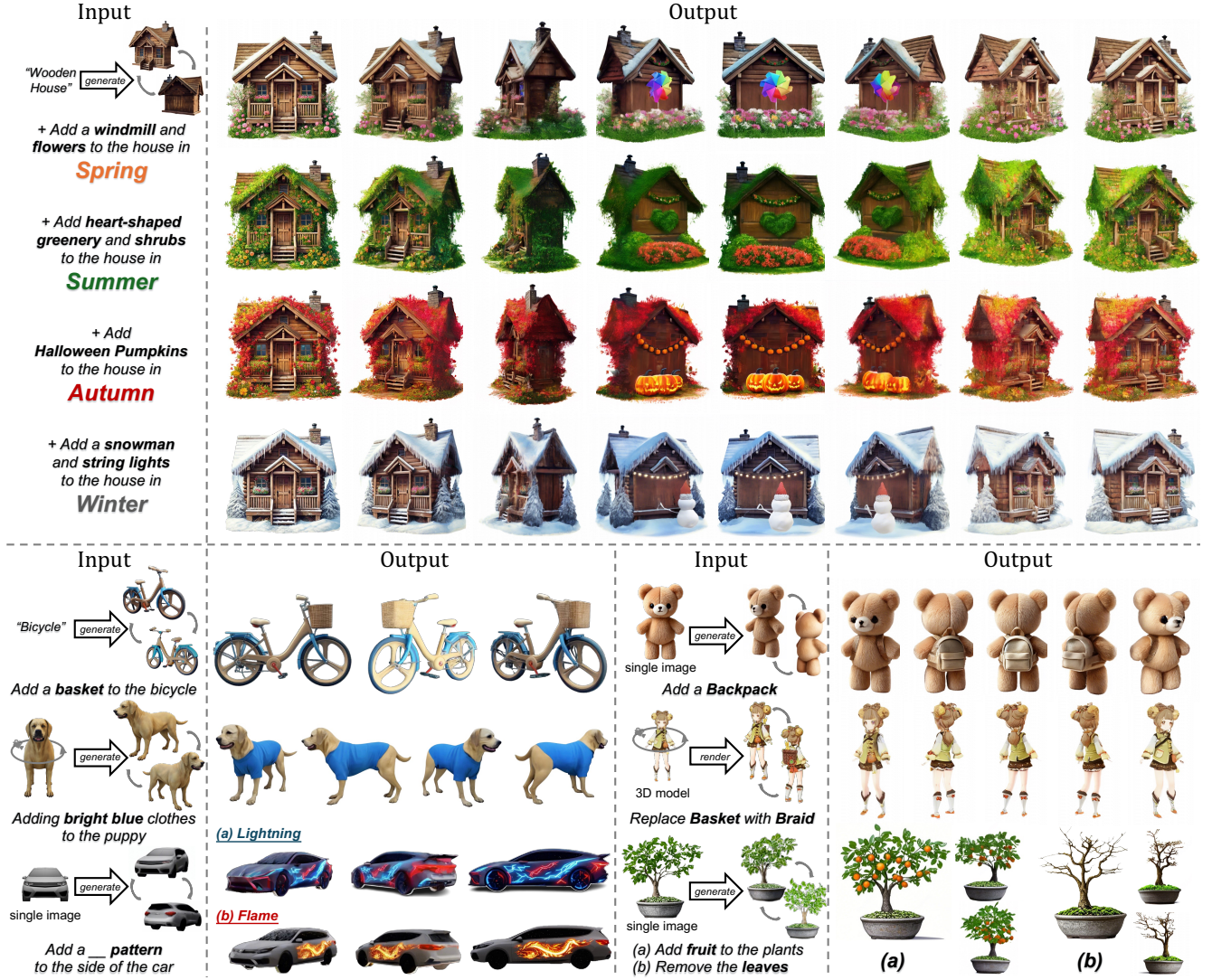


Figure 5. Examples of local element editing with Edit360. Our framework accepts various inputs (text, single images, or 3D models) and editing instructions, showing precise local modifications including element insertion, deletion, and replacement across various subjects.

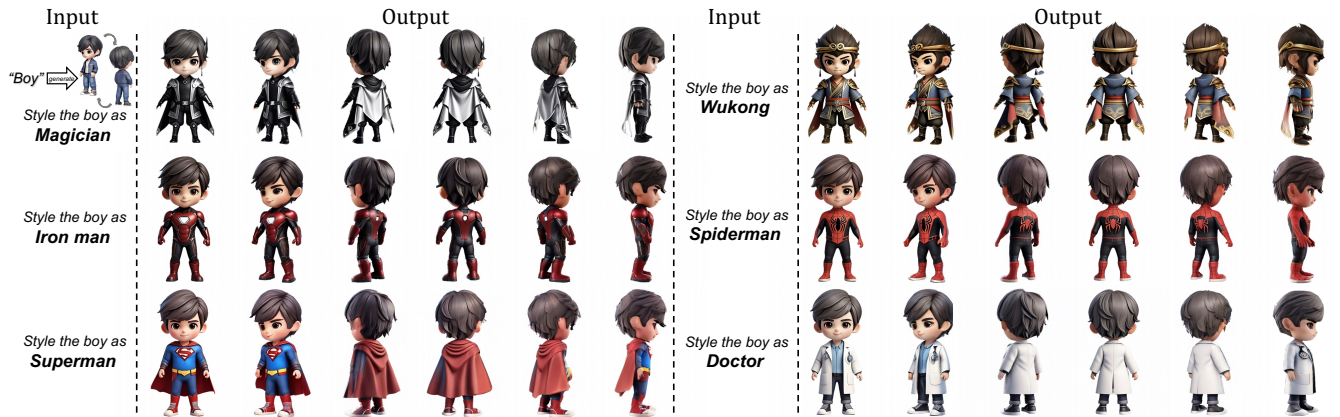


Figure 6. Examples of global style transfer with Edit360. Our method successfully transfers diverse character styles (Magician, Iron Man, Superman, Wukong, Spiderman, and Doctor) while preserving the original character's identity.

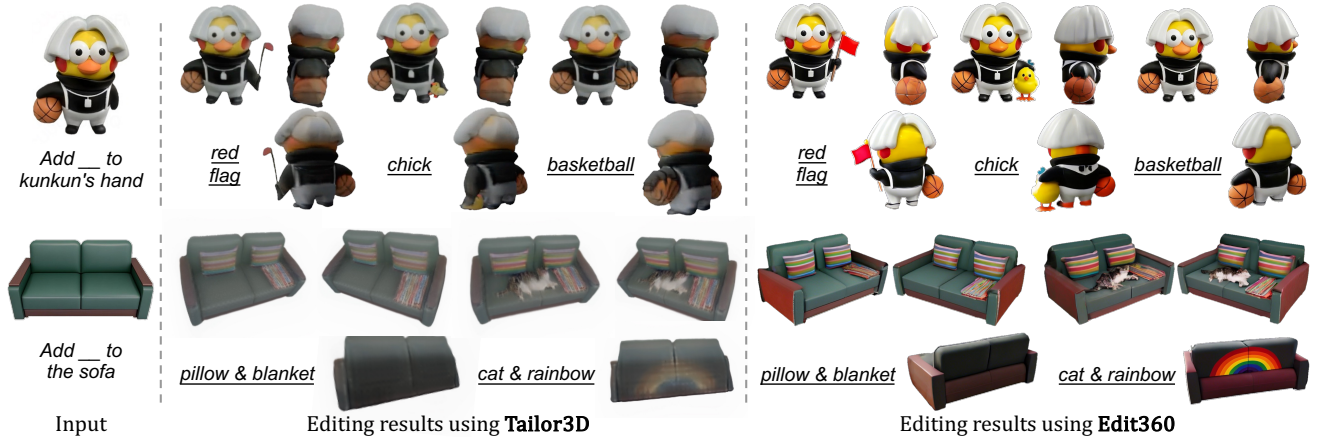


Figure 7. Qualitative comparison of editing results between Tailor3D [48] and our Edit360 framework. Edit360 produces sharper, higher-resolution textures and richer geometric details, resulting in more realistic 3D editing results.

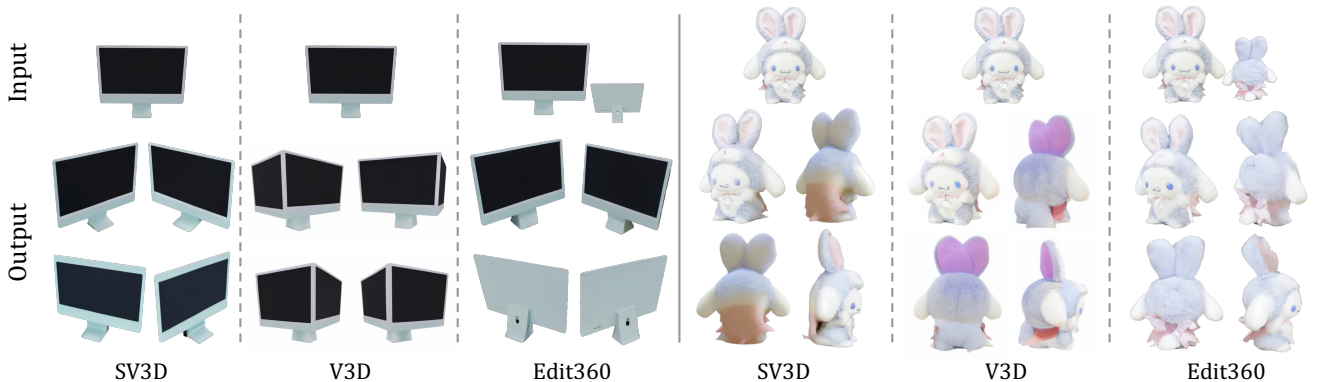


Figure 8. Qualitative comparison between existing V3DMs and our enhanced Edit360 framework. Our method surpasses both SV3D [48] and V3D [6] by avoiding multi-faced Janus problems (e.g., the monitor) and generating richer back details (e.g., the doll’s rear appearance).

our method’s ability to generate novel views using the unseen Google Scanned Objects (GSO)[10] and OmniObject3D [54] datasets. Given the large number of similar objects with minor color variations existed in GSO dataset, we followed SV3D[48], filtering out 300 objects with significant shape differences from the dataset to ensure diversity and minimize redundancy in our evaluation. We generate dense orbit videos based on camera trajectories and compare each generated frame to the corresponding ground truth using multiple metrics: LPIPS [61], PSNR, and SSIM [51] for comprehensive evaluation.

5.2. 3D Asset Editing

Our framework enables precise local editing of diverse 3D assets from arbitrary viewpoints, supporting operations such as element insertion, replacement, and removal. Moreover, it facilitates comprehensive style transformations through specified editing directives.

Local Element Editing. Figure 5 demonstrates our framework’s capability for localized editing through element-level modifications. In the first example, we input a front view of a cabin generated by DALL-E using the prompt

“wooden house” and applied seasonal edits with to create 360-degree view videos. For each season, we add specific elements: a windmill and flowers for spring, heart-shaped greenery and shrubs for summer, Halloween pumpkins for autumn, and both a snowman and string lights for winter. Additionally, we demonstrate the framework’s versatility across various subjects—characters, vehicles, animals, and plants—through precise modifications including accessory addition, component replacement, and element removal.

Global Style Transfer. Edit360 enables global style transfer across 360-degree views by replacing editing instructions with style-specific prompts, while preserving the subject’s identity. As shown in Figure 6, starting from a text-generated boy image, we successfully transform his appearance into various fantasy and superhero characters (Magician, Iron Man, Superman, Wukong, Spiderman, and Doctor) while preserving his distinct facial features.

Comparison in 3D editing task. Tailor3D is a concurrent work that explores extending 2D editing to 3D domain. However, they are constrained by fixed editing viewpoints (front and back views), making it challenging to edit other angles (e.g., side views). Edit360 supports flexible editing

Approach	Geometric	Texture	Overall
Tailor3D	3.32	2.77	3.02
Edit360 (Ours)	4.56	4.49	4.52

Table 1. Comparison of user study ratings between Edit360 and Tailor3D for 3D editing tasks across geometric consistency, texture preservation, and overall performance.

Model	GSO Dataset			OmniObject3D Dataset		
	LPIPS ↓	PSNR ↑	SSIM ↑	LPIPS ↓	PSNR ↑	SSIM ↑
Zero123 [25]	0.13	17.29	0.79	0.17	15.50	0.76
Zero123XL [7]	0.14	17.11	0.78	0.18	15.36	0.75
Stable Zero123 [43]	0.13	18.34	0.78	0.15	16.86	0.77
Free3D [62]	0.15	16.18	0.79	0.16	15.29	0.78
EscherNet [20]	0.13	16.73	0.79	0.17	14.63	0.74
SV3D [48]	0.09	21.14	0.87	0.10	19.68	0.86
Edit-V3D (v^0)	0.09	21.30	0.91	0.10	19.64	0.87
Edit-SV3D (v^0)	0.08	21.65	0.86	0.10	19.77	0.88
Edit-V3D (v^0 & v^i)	0.09	21.42	0.92	0.09	19.98	0.87
Edit-SV3D (v^0 & v^i)	0.07	22.17	0.90	0.08	20.44	0.89
Edit-SV3D (2GT input)	0.06	26.32	0.93	0.07	24.52	0.91

Table 2. Quantitative comparison of our Edit360 framework with recent novel view synthesis methods.

from any viewpoint, and achieves better editing results by selecting anchor views for specific editing tasks. Furthermore, by leveraging rich visual priors from video diffusion models, our method achieves more refined and realistic editing effects. We conduct qualitative comparisons using the same examples shown in their paper, as demonstrated in Figure 7. Edit360 achieves superior geometric structure and richer texture details. Additionally, we conducted a user study to evaluate 3D editing quality, recruiting 50 participants to assess eight editing examples (each presented from four distinct viewpoints). As illustrated in Table 1, evaluators rated our method on a 5-point Likert scale across three dimensions: geometric consistency, texture detail, and overall performance. The results clearly demonstrate the superiority of our approach in these critical aspects.

5.3. Novel Multi-View Synthesis

While Edit360 primarily focuses on 3D editing capabilities, it’s crucial to validate that our framework preserves multi-view consistency when introducing additional view conditions during the editing process. Therefore, we evaluate Edit360’s performance in novel view synthesis tasks, demonstrating that our framework do not compromise the underlying generation capabilities of base V3DM models. As shown in Table 2, we quantitatively compare with some state-of-the-art novel view synthesis methods and two V3DM methods (V3D [6], SV3D [48]), as well as the V3DM methods enhanced with Edit360. For fair comparison, all the single-view input methods utilize a ground-truth front view v^0 as input, an additional anchor view v^i for Edit360 is generated using the original single front-view input V3DM model (where i is a randomly selected frame index from the dense-view sequence).

Additionally, we evaluate Edit360 with a two-view

SPF	CVA	LPIPS ↓	PSNR ↑	SSIM ↑	CLIP-S ↑	MSE ↓
		0.11	20.57	0.83	0.85	0.02
✓		0.08	20.90	0.87	0.85	0.02
✓	✓	0.07	22.17	0.90	0.88	0.02

Table 3. Ablation study on key components of the Edit360: Spatial Progressive Fusion (SPF) and Cross-View Alignment (CVA), demonstrating their individual contributions to performance.

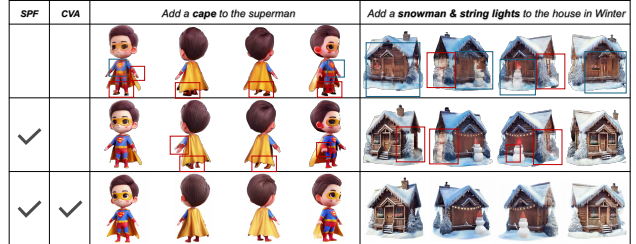


Figure 9. Visual ablations on SPF and CVA: The first row shows results by directly adding features after rotation alignment (Eq. 4). Red boxes indicate inconsistencies, while blue boxes indicate over-smoothing artifacts. With both modules, our method (third row) produces more consistent and detailed results.

ground-truth input setting (“2GT input” in Table 2), where two ground-truth views are provided as input anchor views. This setting reaches a significant performance improvement, highlighting the superior upperbound of our framework when leveraging multi-view ground-truth inputs. The qualitative comparison is shown in Figure 8. We observe that conventional V3DM methods (SV3D [48], V3D [6]) often generate incorrect or overly smooth back views, failing to preserve the complex textures and details present in the front view (e.g., the doll in Figure 8). Additionally, these methods sometimes suffer from the “Janus problem”, where the front-view content is incorrectly repeated in other viewpoints (e.g., the monitor in Figure 8). In contrast, our framework ensures texture consistency across surrounding views by leveraging multi-view inputs (e.g., front and back views).

5.4. Ablation Studies

We present the following ablation studies on the GSO dataset based on the experimental settings outlined in Sec 5.1. As shown in Table 3, we evaluate the impact of two key components: Spatial Progressive Fusion (SPF), and Cross-View Alignment (CVA). The baseline model uses simple linear interpolation with equal weights across all frames. The results highlight the importance of each component in our framework. Additionally, Figure 4 and Figure 9 provide visual ablations to demonstrates the effect of the proposed SPF and CVA modules.

6. Conclusions

In conclusion, Edit360 offers a novel training-free solution for 3D asset editing, enabling precise 360-degree customization based on user-specified instructions. By iden-

tifying the optimal editing views for specific editing tasks, and consistently integrating 2D edits into the entire 3D asset through Spatial Progressive Fusion (SPF) and Cross-View Alignment (CVA), we achieve precise 3D editing. This approach overcomes the limitations of prior methods, facilitating complex editing tasks while maintaining spatial coherence and detail throughout the entire 3D model. With its capacity for detailed and flexible 3D customizations, Edit360 shows great potential for applications in animation, gaming, and virtual reality requiring 3D asset manipulation.

References

- [1] Andreas Blattmann, Tim Dockhorn, Sumith Kulal, Daniel Mendelevitch, Maciej Kilian, Dominik Lorenz, Yam Levi, Zion English, Vikram Voleti, Adam Letts, et al. Stable video diffusion: Scaling latent video diffusion models to large datasets. *arXiv preprint arXiv:2311.15127*, 2023. 2
- [2] Hansheng Chen, Ruoxi Shi, Yulin Liu, Bokui Shen, Jiayuan Gu, Gordon Wetzstein, Hao Su, and Leonidas Guibas. Generic 3d diffusion adapter using controlled multi-view editing, 2024. 3
- [3] Xi Chen, Lianghua Huang, Yu Liu, Yujun Shen, Deli Zhao, and Hengshuang Zhao. Anydoor: Zero-shot object-level image customization. In *CVPR*, 2024. 2
- [4] Yang Chen, Yingwei Pan, Yehao Li, Ting Yao, and Tao Mei. Control3D: Towards Controllable Text-to-3D Generation. In *ACMM*, 2023. 3
- [5] Zhiqin Chen and Hao Zhang. Learning Implicit Fields for Generative Shape Modeling. In *CVPR*, 2019. 3
- [6] Zilong Chen, Yikai Wang, Feng Wang, Zhengyi Wang, and Huaping Liu. V3d: Video diffusion models are effective 3d generators. *arXiv preprint arXiv:2403.06738*, 2024. 2, 3, 4, 5, 7, 8
- [7] Matt Deitke, Ruoshi Liu, Matthew Wallingford, Huong Ngo, Oscar Michel, Aditya Kusupati, Alan Fan, Christian Laforte, Vikram S. Voleti, Samir Yitzhak Gadre, Eli VanderBilt, Aniruddha Kembhavi, Carl Vondrick, Georgia Gkioxari, Kiana Ehsani, Ludwig Schmidt, and Ali Farhadi. Objaverse-XL: A Universe of 10M+ 3D Objects. In *NeurIPS*, 2023. 8
- [8] Matt Deitke, Dustin Schwenk, Jordi Salvador, Luca Weihs, Oscar Michel, Eli VanderBilt, Ludwig Schmidt, Kiana Ehsani, Aniruddha Kembhavi, and Ali Farhadi. Objaverse: A Universe of Annotated 3D Objects. In *CVPR*, 2023. 5
- [9] Matt Deitke, Ruoshi Liu, Matthew Wallingford, Huong Ngo, Oscar Michel, Aditya Kusupati, Alan Fan, Christian Laforte, Vikram Voleti, Samir Yitzhak Gadre, et al. Objaverse-xl: A universe of 10m+ 3d objects. *NeurIPS*, 2024. 2
- [10] Laura Downs, Anthony Francis, Nate Koenig, Brandon Kinman, Ryan Michael Hickman, Krista Reymann, Thomas Barlow McHugh, and Vincent Vanhoucke. Google Scanned Objects: A High-Quality Dataset of 3D Scanned Household Items. In *ICRA*, 2022. 7
- [11] I. Y. Fogel and Dov Sagi. Gabor filters as texture discriminator. In *Biological Cybernetics*, 1989. 5
- [12] Lin Gao, Yu-Kun Lai, Dun Liang, Shu-Yu Chen, and Shihong Xia. Efficient and flexible deformation representation for data-driven surface modeling. In *ACM Transactions on Graphics (TOG)*, 2016. 3
- [13] Lin Gao, Yu-Kun Lai, Jie Yang, Ling-Xiao Zhang, Shihong Xia, and Leif Kobbelt. Sparse data driven mesh deformation. In *IEEE transactions on visualization and computer graphics*, 2019. 3
- [14] Rohit Girdhar, Mannat Singh, Andrew Brown, Quentin Duval, Samaneh Azadi, Sai Saketh Rambhatla, Akbar Shah, Xi Yin, Devi Parikh, and Ishan Misra. Emu video: Factorizing text-to-video generation by explicit image conditioning. *arXiv preprint arXiv:2311.10709*, 2023. 2
- [15] Junlin Han, Filippos Kokkinos, and Philip Torr. Vfusion3d: Learning scalable 3d generative models from video diffusion models. In *ECCV*. Springer, 2025. 3, 5
- [16] Jonathan Ho, AjayN. Jain, and Pieter Abbeel. Denoising diffusion probabilistic models. *NeurIPS*, 2020. 1
- [17] Alec Jacobson, Ilya Baran, Ladislav Kavan, Jovan Popović, and Olga Sorkine. Fast automatic skinning transformations. In *ACM Transactions on Graphics (ToG)*, 2012. 3
- [18] N. Kanopoulos, N. Vasanthavada, and R.L. Baker. Design of an image edge detection filter using the Sobel operator. In *IEEE Journal of Solid-State Circuits*, 1988. 5
- [19] Bernhard Kerbl, Georgios Kopanas, Thomas Leimkühler, and George Drettakis. 3d gaussian splatting for real-time radiance field rendering. In *ACM TOG*, 2023. 4
- [20] Xin Kong, Shikun Liu, Xiaoyang Lyu, Marwan Taher, Xiaojuan Qi, and Andrew J. Davison. Eschernet: A generative model for scalable view synthesis. In *CVPR*, 2024. 8
- [21] Dmytro Kotovenko, Artsiom Sanakoyeu, Pingchuan Ma, Sabine Lang, and Bjorn Ommer. A content transformation block for image style transfer. In *CVPR*, 2019. 2
- [22] Jeong-gi Kwak, Erqun Dong, Yuhe Jin, Hanseok Ko, Shweta Mahajan, and Kwang Moo Yi. Vivid-1-to-3: Novel view synthesis with video diffusion models. In *CVPR*, 2024. 3
- [23] Chen-Hsuan Lin, Jun Gao, Luming Tang, Towaki Takikawa, Xiaohui Zeng, Xun Huang, Karsten Kreis, Sanja Fidler, Ming-Yu Liu, and Tsung-Yi Lin. Magic3d: High-resolution text-to-3d content creation. In *CVPR*, 2023. 2
- [24] Lijuan Liu, Youyi Zheng, Di Tang, Yi Yuan, Changjie Fan, and Kun Zhou. Neuroskinning: Automatic skin binding for production characters with deep graph networks. In *ACM Transactions on Graphics (ToG)*, 2019. 3
- [25] Ruoshi Liu, Rundi Wu, Basile Van Hoorick, Pavel Tokmakov, Sergey Zakharov, and Carl Vondrick. Zero-1-to-3: Zero-shot one image to 3d object. In *ICCV*, 2023. 2, 8
- [26] Steven Liu, Xiuming Zhang, Zhoutong Zhang, Richard Zhang, Jun-Yan Zhu, and Bryan Russell. Editing conditional radiance fields. In *ICCV*, 2021. 3
- [27] Yuan Liu, Chu-Hsing Lin, Zijiao Zeng, Xiaoxiao Long, Lingjie Liu, Taku Komura, and Wenping Wang. Syncdreamer: Generating multiview-consistent images from a single-view image. *ICLR*, abs/2309.03453, 2024. 2
- [28] Thalmann Magnenat, Richard Laperrière, and Daniel Thalmann. Joint-dependent local deformations for hand animation and object grasping. In *Proceedings of Graphics Interface'88*, 1988. 3

- [29] Antoine Mercier, Ramin Nakhli, Mahesh Reddy, Rajeev Yasarla, Hong Cai, Fatih Porikli, and Guillaume Berger. Hexagen3d: Stablediffusion is just one step away from fast and diverse text-to-3d generation. *arXiv preprint arXiv:2401.07727*, 2024. 2
- [30] Gal Metzger, Elad Richardson, Or Patashnik, Raja Giryes, and Daniel Cohen-Or. Latent-nerf for shape-guided generation of 3d shapes and textures. In *CVPR*, 2023. 2
- [31] Yatian Pang, Tanghui Jia, Yujun Shi, Zhenyu Tang, Junwu Zhang, Xinhua Cheng, Xing Zhou, Francis EH Tay, and Li Yuan. Envision3d: One image to 3d with anchor views interpolation. *arXiv preprint arXiv:2403.08902*, 2024. 3, 5
- [32] Jeong Joon Park, Peter Florence, Julian Straub, Richard Newcombe, and Steven Lovegrove. DeepSDF: Learning Continuous Signed Distance Functions for Shape Representation. In *CVPR*, 2019. 3
- [33] Ben Poole, Ajay Jain, Jonathan T Barron, and Ben Mildenhall. Dreamfusion: Text-to-3d using 2d diffusion. In *ICLR*, 2023. 2
- [34] Zhangyang Qi, Yunhan Yang, Mengchen Zhang, Long Xing, Xiaoyang Wu, Tong Wu, Dahua Lin, Xihui Liu, Jiaqi Wang, and Hengshuang Zhao. Tailor3d: Customized 3d assets editing and generation with dual-side images. *arXiv preprint arXiv:2407.06191*, 2024. 3
- [35] Apoorva Rauniyar, Aryan Raj, Ashish Kumar, Ashish Kumar Kandu, Astha Singh, and Anjani Gupta. Text to Image Generator with Latent Diffusion Models. In *CICTN*, 2023. 4, 5
- [36] Robin Rombach, Andreas Blattmann, Dominik Lorenz, Patrick Esser, and Bjorn Ommer. High-Resolution Image Synthesis with Latent Diffusion Models. In *CVPR*, 2022. 1
- [37] Nataniel Ruiz, Yuanzhen Li, Varun Jampani, Yael Pritch, Michael Rubinstein, and Kfir Aberman. Dreambooth: Fine tuning text-to-image diffusion models for subject-driven generation. In *CVPR*, 2023. 2
- [38] Chitwan Saharia, William Chan, Saurabh Saxena, Lala Li, Jay Whang, Emily L Denton, Kamyar Ghasemipour, Raphael Gontijo Lopes, Burcu Karagol Ayan, Tim Salimans, et al. Photorealistic text-to-image diffusion models with deep language understanding. *NeurIPS*, 2022. 1
- [39] Thomas W Sederberg and Scott R Parry. Free-form deformation of solid geometric models. In *ACM SIGGRAPH Computer Graphics*, 1986. 3
- [40] Yang Song, Jascha Sohl-Dickstein, Diederik P Kingma, Abhishek Kumar, Stefano Ermon, and Ben Poole. Score-based generative modeling through stochastic differential equations. *arXiv preprint arXiv:2011.13456*, 2020. 1
- [41] Olga Sorkine. Laplacian mesh processing. In *Eurographics (State of the Art Reports)*, 2005. 3
- [42] Olga Sorkine and Marc Alexa. As-rigid-as-possible surface modeling. In *Symposium on Geometry processing*, 2007. 3
- [43] StabilityAI. Stable Zero123. <https://stabilityai.com/stable-zero123>, 2023. Accessed: 2023-XX-XX. 8
- [44] Robert W Sumner, Matthias Zwicker, Craig Gotsman, and Jovan Popović. Mesh-based inverse kinematics. In *ACM transactions on graphics (TOG)*, 2005. 3
- [45] Qingyang Tan, Lin Gao, Yu-Kun Lai, and Shihong Xia. Variational autoencoders for deforming 3d mesh models. In *CVPR*, 2018. 3
- [46] Shitao Tang, Jiacheng Chen, Dilin Wang, Chengzhou Tang, Fuyang Zhang, Yuchen Fan, Vikas Chandra, Yasutaka Furukawa, and Rakesh Ranjan. Mvdifffusion++: A dense high-resolution multi-view diffusion model for single or sparse-view 3d object reconstruction. In *ECCV*, 2024. 2
- [47] Vikram Voleti, Alexia Jolicoeur-Martineau, and Chris Pal. Mcvd-masked conditional video diffusion for prediction, generation, and interpolation. *NeurIPS*, 35, 2022. 2
- [48] Vikram Voleti, Chun-Han Yao, Mark Boss, Adam Letts, David Pankratz, Dmitry Tochilkin, Christian Laforte, Robin Rombach, and Varun Jampani. Sv3d: Novel multi-view synthesis and 3d generation from a single image using latent video diffusion. In *ECCV*, 2024. 2, 3, 4, 5, 7, 8
- [49] Haofan Wang, Matteo Spinelli, Qixun Wang, Xu Bai, Zekui Qin, and Anthony Chen. Instantstyle: Free lunch towards style-preserving in text-to-image generation. *arXiv preprint arXiv:2404.02733*, 2024. 2
- [50] Peng Wang, Lingjie Liu, Yuan Liu, Christian Theobalt, Taku Komura, and Wenping Wang. NeuS: Learning Neural Implicit Surfaces by Volume Rendering for Multi-view Reconstruction. In *NeurIPS*, 2021. 4
- [51] Zhou Wang, A.C. Bovik, H.R. Sheikh, and E.P. Simoncelli. Image quality assessment: from error visibility to structural similarity. In *IEEE Transactions on Image Processing*, 2004. 7
- [52] Zhengyi Wang, Cheng Lu, Yikai Wang, Fan Bao, Chongxuan Li, Hang Su, and Jun Zhu. Prolificdreamer: High-fidelity and diverse text-to-3d generation with variational score distillation. *NeurIPS*, 2024. 2
- [53] Daniel Watson, William Chan, Ricardo Martin-Brualla, Jonathan Ho, Andrea Tagliasacchi, and Mohammad Norouzi. Novel view synthesis with diffusion models. *arXiv preprint arXiv:2210.04628*, 2022. 2
- [54] Tong Wu, Jiarui Zhang, Xiao Fu, Yuxin Wang, Jiawei Ren, Liang Pan, Wayne Wu, Lei Yang, Jiaqi Wang, Chen Qian, et al. Omniobject3d: Large-vocabulary 3d object dataset for realistic perception, reconstruction and generation. In *CVPR*, 2023. 7
- [55] Zhan Xu, Yang Zhou, Evangelos Kalogerakis, Chris Landreth, and Karan Singh. RigNet: Neural Rigging for Articulated Characters. In *SIGGRAPH*, 2020. 3
- [56] Bangbang Yang, Yinda Zhang, Yinghao Xu, Yijin Li, Han Zhou, Hujun Bao, Guofeng Zhang, and Zhaopeng Cui. Learning object-compositional neural radiance field for editable scene rendering. In *ICCV*, 2021. 3
- [57] Wang Yifan, Noam Aigerman, Vladimir G Kim, Siddhartha Chaudhuri, and Olga Sorkine-Hornung. Neural cages for detail-preserving 3d deformations. In *CVPR*, 2020. 3
- [58] Yu-Jie Yuan, Yu-Kun Lai, Tong Wu, Lin Gao, and Ligang Liu. A revisit of shape editing techniques: From the geometric to the neural viewpoint. In *Journal of Computer Science and Technology*, 2021. 3
- [59] Yu-Jie Yuan, Yang-Tian Sun, Yu-Kun Lai, Yuewen Ma, Rongfei Jia, and Lin Gao. Nerf-editing: geometry editing of neural radiance fields. In *CVPR*, 2022. 3

- [60] Lvmin Zhang, Anyi Rao, and Maneesh Agrawala. Adding Conditional Control to Text-to-Image Diffusion Models. In *ICCV*, 2023. [1](#), [2](#)
- [61] Richard Zhang, Phillip Isola, Alexei A. Efros, Eli Shechtman, and Oliver Wang. The Unreasonable Effectiveness of Deep Features as a Perceptual Metric. In *CVPR*, 2018. [7](#)
- [62] Chuanxia Zheng and Andrea Vedaldi. Free3D: Consistent Novel View Synthesis without 3D Representation. In *CVPR*, 2024. [8](#)